Published in final edited form as:
Nano Lett. 2009 December ; 9(12): 4412–4416. doi:10.1021/nl902709m.

Polymeric Nanoparticle-Based Activatable Near-Infrared Nanosensor for Protease Determination In Vivo

Seulki Lee[†,‡,⊥], **Ju Hee Ryu**[†,⊥], **Kyeongsoon Park**[†], **Aeju Lee**[†], **Seung-Young Lee**[†], **In-Chan Youn**[†], **Cheol-Hee Ahn**[§], **Soon Man Yoon**[‖], **Seung-Jae Myung**[‖], **Dae Hyuk Moon**[‖], **Xiaoyuan Chen**[‡], **Kuiwon Choi**[†], **Ick Chan Kwon**[†], and **Kwangmeyung Kim**[*,†]
Biomedical Research Center, Korea Institute of Science and Technology, 39-1 Hawolgok-dong, Seongbuk-gu, Seoul 136-791, Korea, National Institute of Biomedical Imaging and Bioengineering, National Institutes of Health, 9000 Rockville Pike, Bethesda, Maryland 20892, School of Materials Science and Engineering, Seoul National University, 599 Gwanangno, Gwanak-gu, Seoul 151-742, Korea, and Asan Medical Center, University of Ulsan College of Medicine, 388-2 Pungnap2-dong, Songpa-gu, Seoul 138-736, Korea

Abstract

We report here a new protease activatable strategy based on a polymer nanoparticle platform. This nanosensor delivers chemically labeled matrix metalloproteinase (MMP)-activatable fluorogenic peptides to the specific MMPs of interest in vivo. Intravenous administration of the nanosensor in an MMP-positive SCC-7 xenograft tumor and a colon cancer mouse model verified the enzyme specificity of the nanosensor in vivo. The design platform of the nanosensor is flexible and can be fine-tuned for a wide array of applications such as the detection of biomarkers, early diagnosis of disease, and monitoring therapeutic efficacy.

Recent interdisciplinary research at the interface of optical molecular imaging science and nanotechnology has generated novel imaging probes with unique design strategies.[1–3] However, most in vivo applications are hampered by insufficient resolution at the target site. This limitation is a product of low fluorescent signal amplification and specificity of the probe for the event of interest. Various recently developed imaging probes described by the term “fluorescent signal activation methods”, which are also known as activatable probes, have shown promising results.[4,5] However, many of these probes are thus far limited in usefulness in vivo, mainly because of low target-to-background ratios or lack of stability in physiological conditions after intravenous injection.[4] Therefore, the development of more sophisticated and reliable activatable probes capable of boosting the intensity of fluorescent signals at the region of interest (ROI) with specific target recognition properties is urgently needed.

Proteases are the most important and extensively studied enzymes owing to their various regulatory roles in biological processes.[6] A number of recent advances in noninvasive optical imaging have enabled monitoring of protease activity.[7–10] These methods mostly

[*]To whom correspondence should be addressed. Phone: +82-2-958-5916. Fax+82-2-958-5902. kim@kist.re.kr.
[†]Korea Institute of Science and Technology.
[‡]National Institute of Biomedical Imaging and Bioengineering.
[§]Seoul National University.
[‖]University of Ulsan College of Medicine.
[⊥]These authors contributed equally to this work.

Supporting Information Available: Details of synthesis and experimental methods. This material is available free of charge via the Internet at http://pubs.acs.org.

rely on a peptide substrate that becomes fluorescent in vivo. While they are valuable, probes that are designed only based on substrates might be limited by their overall lack of region specificity (i.e., tumors).

We report here a new protease activatable strategy based on a polymeric nanoparticle platform. We describe a self-assembled polymeric nanoparticle-based activatable probe (nanosensor, NS) that can be used as an efficient activatable optical contrast agent for imaging of various protease-associated diseases in vivo after intravenous injection. The NS consists of strongly quenched matrix metalloproteinase (MMP)-specific near-infrared (NIR) fluorogenic peptides on the surface of tumor-homing polymeric nanoparticles as a carrier. MMPs are a family of zinc-dependent proteins that play essential roles in many aspects of biology.[11] Since expression of MMPs are significantly involved in cancer progression and certain inflammatory diseases, a variety of imaging modalities are utilized for the detection and imaging of MMPs in vivo. As proof-of-concept, in vivo imaging of pathologies with MMP-related diseases, including an MMP-positive xenografted tumor and colon cancer mouse model, were performed. Intravenous administration of the NS verified the MMP-associated disease region with high specificity with minimal background signals that correlated with levels of active MMPs in those tissues. These results were confirmed in vivo and ex vivo imaging and immunohisotology methods. The NS represents a new tool for investigation of the role of proteases in pathophysiology, for identification of therapeutic biomarkers, and for monitoring therapeutic efficacy in vivo.

We developed an NS consisting of a self-assembled chitosan nanoparticle (CNP) and an activatable dark-quenched fluorogenic peptide Cy5.5 (NIR dye)–peptide substrate, which is quenched by the NIR dark quencher, BHQ-3[12] (Figure 1). It was hypothesized that chemically labeled activatable probes on the surface of nanoparticles induce a higher specificity and sensitivity of the probe in vivo, since the nanoparticles can deliver the probe effectively to the disease sites (i.e., tumor region) by the enhanced permeation retention (EPR) effect[13] and because the peptide substrate-mediated fluorescence labeling of the nanoparticles can be strongly dual-quenched by both the dye-dark quencher and NIR dye–dye self-quenching mechanisms (Figure 1A). When the NS is exposed to the specific MMP of interest, cleavage of the NIR-dye substrate occurs due to specific substrate recognition by the MMPs; this is manifest in the form of a pronounced NIR fluorescence signal recovery due to dequenching of the dye (Figure 1B).

To demonstrate our rationale, we prepared CNPs that were labeled with the activatable fluorogenic peptide, Cy5.5-Gly-Pro-Leu-Gly-Val-Arg-Gly-Lys(BHQ3)-Gly-Gly (Figures S1 and S2; see the Supporting Information). In the probe, the core specific substrate, Pro-Leu-Gly-Val-Arg-Gly,[14] shows selectivity for various MMPs (Figure 1C). To prepare the CNPs, glycol chitosan (molecular weight (MW) 250 kDa) was modified with 150 ± 5 molecules of hydrophobic 5β-cholanic acid per polymer.[15] Activatable fluorogenic peptide was synthesized by standard solid-phase Fmoc peptide chemistry as previously described.[7] When the CNPs were dissolved in aqueous solution, they spontaneously self-assembled into stable nanoparticles under sonification. These CNPs were labeled with the dark-quenched fluorogenic peptides in the presence of the chemical catalyst. The reaction mixtures were repeatedly dialyzed against distilled water and concentrated by Amicon Ultracell-10K (Millipore). The desired NS was further purified by fast-performance liquid chromatography (GE AKTA Purifier System), size-exclusion chromatography using Superdex TM200 10/300GL, and lyophilized (99.0% purity; Figure S3; see the Supporting Information). Conjugation of the dark-quenched fluorogenic peptides to the CNPs was confirmed by the measurement the absorption intensity of BHQ-3 (650 nm) using an ultraviolet–visible (UV–vis) spectrometer and the zeta potential change before and after modification of the nanoparticles. From the measurement of absorption intensity produced from the NS, we

estimated that 30 ± 2 peptides were attached to the CNPs. In addition, the positively charged amine groups on the CNP surface showed reduction of surface potential an average of + 24 mV to + 13 mV after conjugation, suggesting the charge neutralization of amine groups after conjugation with peptides. Transmission electron microscopy (TEM) revealed that the NSs were spherical and approximately 250 nm in diameter (Figure S4; see the Supporting Information). The probes were well dispersed in the reaction buffer (100 mM Tris, 5 mM calcium chloride, 200 mM NaCl, 0.1% Brij, pH 7.5), and NIR fluorescence signals were completely quenched when visualized with a Kodak Image Station 4000MM equipped with filter systems for Cy5.5. (Figure S4; see the Supporting Information). Furthermore, increased NS concentrations did not affect the background fluorescence signal (Figure 2A). When the NS was treated with MMP-2 (14 nmol/L) in the reaction buffer at 37 °C for 60 min, fluorescence signals were recovered depending on the NS concentrations, indicating that the approach enabled significantly low background to be amplified by the MMPs, thereby resulting in highly sensitive detection. The enzyme selectivity of the NS was investigated in vitro by incubating a fixed concentration of the probe (2.5 μg/mL) in a cuvette containing the reaction buffer and 14 nmol/L of activated MMP-2, 3, 7, 9, or 13 at 37 °C for 80 min. Spectrofluormetry clearly demonstrated that significant time-dependent recovery of the fluorescence signals occurred against MMP-2, 9, and 13 (11.1, 2.5, 1.1, 8.4, and 15.4-fold for MMP-2, 3, 7, 9, and 13, respectively) (Figure 2B). In addition, the probe showed a proportional relationship between recovered fluorescence signals and different MMP-2 concentrations (0.7, 1.75, 3.5, 7, and 14 nmol/L) ($r^2 = 0.99$), whereas the fluorescence signal was inhibited in the presence of the MMP-2/9 inhibitor, SB-3CT[16] (Figure 2C). These observations were further confirmed and visualized through fluorescence imaging. Potential biological toxicity was evaluated in SCC7 (squamous cell carcinoma) cells, and an in vitro cytotoxicity test revealed that the NS was nontoxic (Figure 2D). Taken together, the systemic validation of the NS in vitro indicates that it could be used for quantitative and visual analysis of MMP activity.

We investigated the potential use of NS in vivo using small animal fluorescence tomography configured for NIR fluorescence probe detection (excitement and emission wavelengths of 670 and 700 nm, respectively) (see the Supporting Information). First, MMP-2/9-positive SCC7 tumor-bearing mice were selected as an animal model.[14] NS (100 μg/100 μL phosphate-buffered saline (PBS)/mouse) was intravenously injected into the mice either directly or following pretreatment with MMP-2/9 inhibitor. Figure 3A shows typical serial images of mice obtained for 2 h after the intravenous injection of the probe. The probe provided a high NIR fluorescence signal in MMP-positive tumor-bearing mice and enabled clear visualization of tumors. In contrast, the fluorescence signal from the tumor was significantly reduced when the MMP-2/9 inhibitor was intratumorally administered 30 min before the probe injection. The ratios of the ROI of the tumor to that of the normal region (T/N) are depicted in Figure 3B (T/N: 15.4 ± 1.8 and 6.4 ± 1.4 without and with inhibitor, respectively, $P < 0.001$). To further evaluate the increased NIR fluorescence signals in the tumor region, tumors and other organs were excised immediately after in vivo imaging and analyzed using a Kodak Image Station (Figure 3C). As expected, activated NS was specifically detected in the tumors, and the total NIR fluorescence of the excised tumor treated with the NS was stronger than that of MMP inhibitor-treated tumor. To determine the depth profile of activated NS in the tumor, NIR fluorescence images were constructed in slices cut along the *z*-axis (depth of 0–7 mm), and two-dimensional images allowed the longitudinal monitoring of fluorescence distribution in the tumors (Figure 3D). Selective tumor sections were also analyzed by NIR fluorescence microscopy and immunohistochemistry (IHC) (Figure 3E). Fluorescence microscopy images showed a significant difference between the two groups, consistent with in vivo imaging. Hematoxylin and eosin (H&E) and anti-MMP-2 antibody staining revealed SCC7 carcinoma and strong expression of MMP-2 in SCC7 tumors. Next, we determined whether the NS could be used

to differentiate various stages of tumors in vivo. To distinguish treatment response within different tumor sizes, mice with SCC7 tumor masses of nine different sizes (3.5–381.5 mg) were intravenously injected with the NS. The animals were sacrificed 2 h postinjection, and tumors were excised and analyzed using a Kodak Image Station. Figure 3F shows a typical image of the differently sized excised tumors (3.5, 66.8, 172.9, and 381.5 mg). The overall signals proportionally increased depending on the size of tumors. NS was able to image an early stage tumor as small as several milligrams. To further confirm that signals observed in tumor images were due to the MMP activity, we performed biochemical analysis. To determine MMP-2/9 activities in tumors, tissues were collected and homogenized, and normalized protein samples were analyzed by gelatin zymograms.[17] The overall relative MMP-2/9 activities observed by gel analysis strongly correlated with the intensity of the NIR signals obtained in the tumor images ($r^2 = 0.91$), which suggests that the signals observed in different tumors were due to specific NS recognition of MMPs. The control imaging experiments were also carried out after the intravenous injection of the unbound dark-quenched peptide (without nanoparticle) and the CNP-Cy5.5 (nonquenched nanoparticle). As expected, the NS showed pronounced NIR fluorescence signals in the tumor region compared to other samples, and the result evidently supports the role of nanoparticles as the carrier system (Figure S5; see the Supporting Information). To determine whether the NS could be used to image MMP activities within other tumor types, we studied imaging responses using a colon tumor mouse model. The MMP-9-positive colon tumors were developed in the middle and distal colon of mice treated with azoxymethane (AOM), as described previously[18] (Figure 4A). Tumor-bearing mice were intravenously injected with NS (100 μg/100 μL PBS/mouse), and mice were sacrificed after 2 h injection. The NIR ex vivo image demonstrated that all tumors obtained high fluorescence signals compared with adjacent mucosa (Figure 4A). H&E staining revealed well-differentiated carcinomas, and IHC was positive for MMP-9 expression throughout the tumors, in contrast to the negative finding in the normal mucosa (Figure 4B). Overall, our data support the notion that NS can be used for NIR fluorescence imaging of MMP activity in a living animal.

Proteases including MMPs are among the most studied enzyme families due to their involvement in the regulation of diverse disease processes and their potential value as biomarkers and therapeutic targets. In this study, we present a new class of polymeric nanoparticle platform-based protease-activatable probes that allow noninvasive imaging of the specific MMPs of interest *in vivo*. The design platform of the NS is flexible and fine-tunable for a wide array of applications such as detection of biomolecules, early diagnosis of disease, and monitoring therapeutic efficacy in vivo. In addition, activatable fluorogenic peptide can be replaced in therapeutic drugs (i.e., chemotherapeutic agents) to allow both imaging and therapy. Work on the development of theranostic nanoplatforms is currently underway and will likely lead to improved utility for these techniques in the near future.

Supplementary Material

Refer to Web version on PubMed Central for supplementary material.

Acknowledgments

This work was financially supported by the Real-Time Molecular Imaging Project, Pioneer Research Program, and Global Research Laboratory Project of MEST and by a grant to the Intramural Research Program of the KIST, and by a grant (A062254) of the Korea Health 21 R&D Project.

References

1. Luker GD, Luker KE. J Nucl Med. 2008; 49:1. [PubMed: 18077528]

2. Pierce MC, Javier DJ, Richards-Kortum R. Int J Cancer. 2008; 123:1979. [PubMed: 18712733]
3. Lee S, Chen X. Mol Imaging. 2009; 8:87. [PubMed: 19397854]
4. Lee S, Park K, Kim K, Choi K, Kwon IC. Chem Commun (Cambridge, UK). 2008:4250.
5. Stefflova K, Chen J, Zheng G. Front Biosci. 2007; 12:4709. [PubMed: 17485407]
6. Edwards DR, Murphy G. Nature. 1998; 394:527. [PubMed: 9707109]
7. Lee S, Park K, Lee SY, Ryu JH, Park JW, Ahn HJ, Kwon IC, Youn IC, Kim K, Choi K. Bioconjugate Chem. 2008; 19:1743.
8. Blum G, von Degenfeld G, Merchant MJ, Blau HM, Bogyo M. Nat Chem Biol. 2007; 3:668. [PubMed: 17828252]
9. Ntziachristos V, Tung CH, Bremer C, Weissleder R. Nat Med. 2002; 8:757. [PubMed: 12091907]
10. Zheng G, Chen J, Stefflova K, Jarvi M, Li H, Wilson BC. Proc Natl Acad Sci USA. 2007; 104:8989. [PubMed: 17502620]
11. Egeblad M, Werb Z. Nat Rev Cancer. 2002; 2:161. [PubMed: 11990853]
12. Johansson MK, Cook RM. Chemistry. 2003; 9:3466. [PubMed: 12898673]
13. Matsumura Y, Maeda H. Cancer Res. 1986; 46:6387. [PubMed: 2946403]
14. Lee S, Cha EJ, Park K, Lee SY, Hong JK, Sun IC, Kim SY, Choi K, Kwon IC, Kim K, Ahn CH. Angew Chem, Int Ed Engl. 2008; 47:2804. [PubMed: 18306196]
15. Hyung Park J, Kwon S, Lee M, Chung H, Kim JH, Kim YS, Park RW, Kim IS, Bong Seo S, Kwon IC, Young Jeong S. Biomaterials. 2006; 27:119. [PubMed: 16023198]
16. Ikejiri M, Bernardo MM, Bonfil RD, Toth M, Chang M, Fridman R, Mobashery S. J Biol Chem. 2005; 280:33992. [PubMed: 16046398]
17. Mook OR, Van Overbeek C, Ackema EG, Van Maldegem F, Frederiks WM. J Histochem Cytochem. 2003; 51:821. [PubMed: 12754293]
18. Nambiar PR, Girnun G, Lillo NA, Guda K, Whiteley HE, Rosenberg DW. Int J Oncol. 2003; 22:145. [PubMed: 12469197]

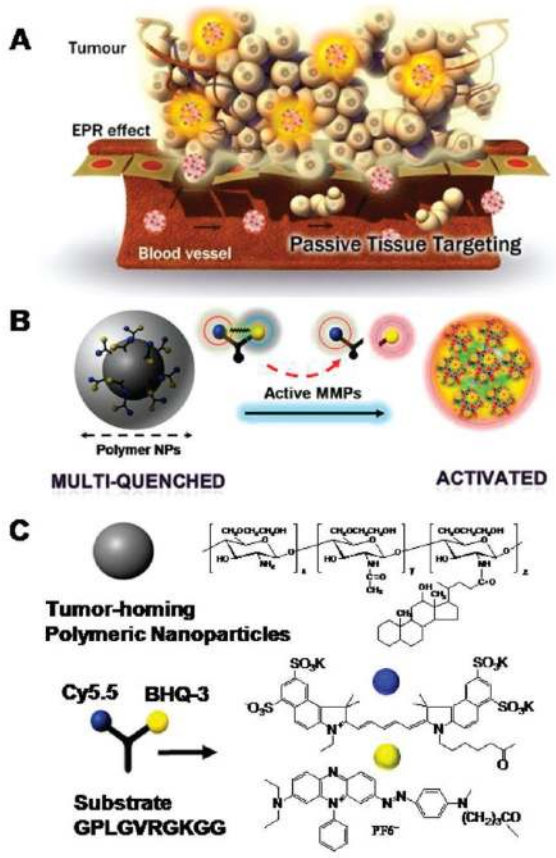

Figure 1.

(A) Schematic diagram of the MMP-sensitive NS. Nanoparticles can deliver multiquenched fluorogenic peptide efficiently to the target site by the EPR effect. When MMPs meet the NS at the site of disease, cleavage of the fluorogenic peptide occurs owing to specific substrate recognition by the MMPs, manifest in the form of pronounced NIR fluorescence signal recovery due to dequenching of the dye. (B) MMP-sensitive NS. Because of the efficient NIR fluorescence quenching ability of the quencher (BHQ-3) and self-quenching of the Cy5.5 dye itself, fluorogenic peptides that are chemically conjugated on the surface of nanoparticles are in the strongly multiquenched state. After cleavage of the substrate by MMPs, NIR fluorescence dyes are released from nanoparticles and fluoresce brightly. (C) Chemical structures of polymeric nanoparticles and MMP-sensitive fluorogenic peptide.

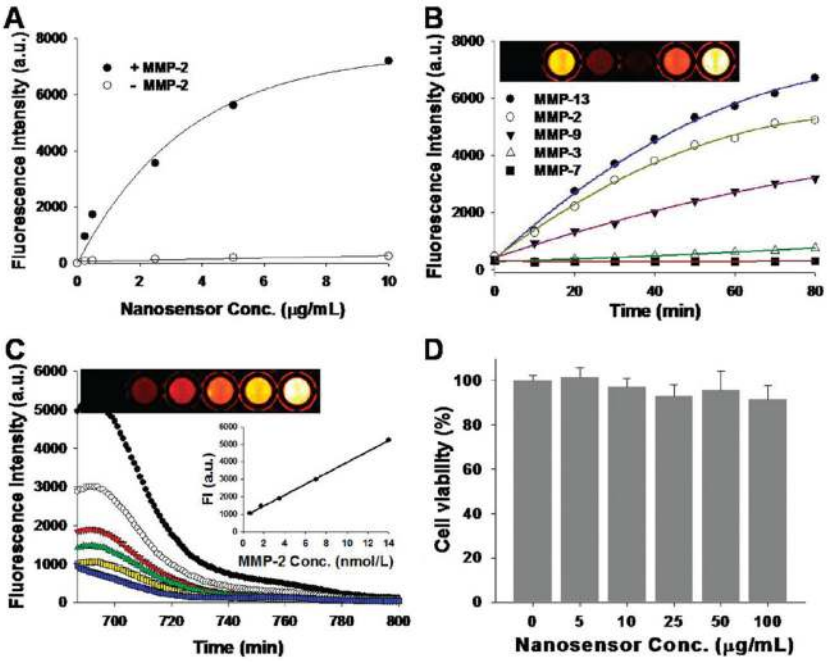

Figure 2.

(A) Quenching properties and recovery of NIR fluorescence intensities in various concentrations of the NS with or without addition of activated MMP-2. MMP specificity of the NS in solution (B,C). (B) Fluorescence emission kinetic spectra of the NS in the presence of various stimuli (MMP-2, 3, 7, 9 and 13, 14 nmol/L) following a 80 min incubation at 37 °C. Top: fluorescence image sections of a 96-well microplate containing different combinations. (C) Fluorescence emission spectra of the NS in the presence of various concentrations of activated MMP-2 (0.7, 1.75, 3.5, 7, 14 nmol/L) and MMP-2 (14 nmol/L) with MMP-2 inhibitor (blue line) following a 80 min incubation at 37 °C. Inset: MMP-2 standard curve; top: corresponding fluorescence image sections of a 96-well microplate. (D) In vitro cellular toxicity of the NS estimated with the MTT assay in SCC7 cells.

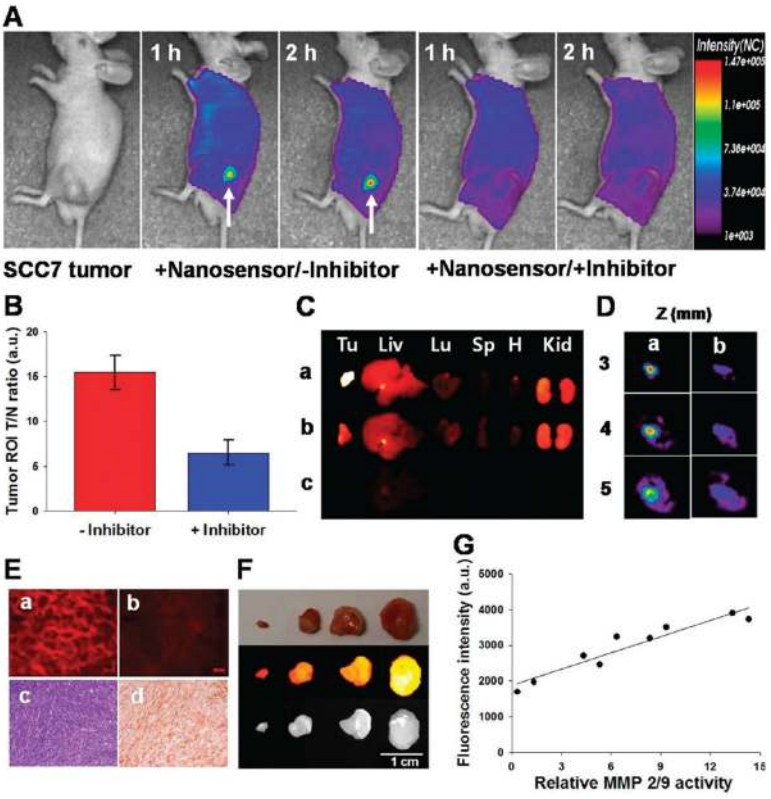

Figure 3.

(A) In vivo NIR fluorescence tomographic images of subcutaneous SCC7 tumor-bearing mice after intravenous injection of the NS with or without the inhibitor. Only tumors injected with the NS without inhibitor were clearly visualized. (B) Tumor ROI and T/N. (C) NIR fluorescence images of excised SCC7 tumor and organs (Tu: tumor; Liv: liver; Lu: lung; Sp: spleen; H: heart; Kid: kidney). NS-treated animals with (a) and without (b) the inhibitor, and saline-treated animals (c). (D) Two-dimensional slices of the tumor images from Figure 3A reconstructed in the *z* direction (3–5 mm). (E) a,b: NIR fluorescence microscopy of SCC7 tumors injected with NS that were left untreated (a) or treated (b) with the inhibitor. Immunohistology analysis of SCC7 tumors. c: H&E stain; d: IHC of MMP-2 protein expression in a SCC7 tumor section counterstained with primary antibody for MMP-2. (F) NIR fluorescence images of excised NS-treated SCC7 tumors from mice with different size tumors. (G) Correlation between tumor grades (total fluorescence intensity) and the relative MMP-2/9 activity of excised SCC7 tumors.

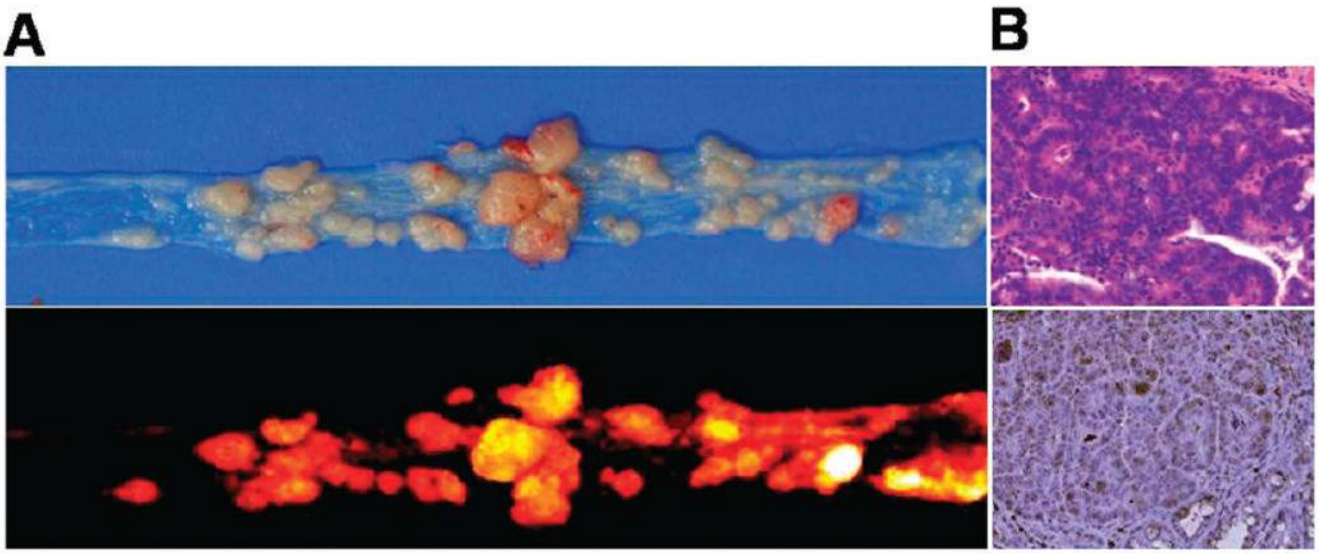

Figure 4.
(A) Upper: photo image of colon tumors from an A/J mouse treated with AOM. Lower: NIR fluorescence image of colon tumors after intravenous injection of the NS. (B) Immunohistology analysis of colon tumors. Upper: H&E stain; lower: IHC of MMP-9 protein expression in a colon tumor section counterstained with primary antibody for MMP-9.